

NEW APPROACH IN ANALYTICAL WORKFLOW TO ACCURATELY
CHARACTERIZE HETEROGENEOUS CARBONATES USING
NON-DESTRUCTIVE TRACERS

A Thesis

by

AMRESH CHAND

Submitted to the Office of Graduate and Professional Studies of
Texas A&M University
in partial fulfillment of the requirements for the degree of

MASTER OF SCIENCE

Chair of Committee,	Hisham A. Nasr-El-Din
Committee Members,	Jerome J. Schubert
	Mahmoud El-Halwagi
Head of Department,	A. Daniel Hill

December 2017

Major Subject: Petroleum Engineering

Copyright 2017 Amresh Chand

ABSTRACT

The main goal of this research is to compare and understand the efficiency of the numerical methods by comparing them with experimental data obtained from coreflood non-destructive tracer experiments on 6 different carbonate cores. Commercial simulation software is used to compare the numerical and experimental tracer concentration profiles and identifying the influencing parameters for history matching.

Six different types of carbonate cores 6 in.-length and 1.5 in. - diameter were obtained from different outcrop cores, with varying pore scale heterogeneity. 8 wt% potassium chloride (KCl) will be used as the non-destructive tracer in all the experiments. After characterizing the carbonates and tracer used in the experiments using standard coreflood procedures, concentration profiles were plotted against time (pore volume tracer injected). Computed tomography (CT) scan was performed on the core samples and single porosity based on the scans was used in the simulation studies. Detailed history matching and sensitivity studies have been carried out thoroughly via commercial simulator, to validate the experimental data and create an accurate model for further analysis.

The ultimate goal of this proposed research is to devise a new analytical workflow to analyze and interpret the effect of heterogeneity in the carbonates using non-destructive tracers and a numerical simulator.

To my parents, sister and family.

ACKNOWLEDGEMENTS

Prima facie, I am grateful to God for the good health and wellbeing that were necessary to complete my thesis.

I wish to express my sincere thanks to Dr. Hisham A. Nasr-El-Din, for his esteemed guidance and support to me during my period of study at Texas A&M University ,by granting me access to all the resources required to learn and apply the knowledge in completing my research, and also particularly for his interest and care in my welfare. His constant motivation is highly responsible for my success.

I thank my committee member, Dr. Jerome J Shubert, who imparted his experience and knowledge and guidance which gave me great confidence in my work.

I thank my committee member, Dr. Mahmoud El-Halwagi, for agreeing to be a part of my committee, and for his constant encouragement to work on my project.

I am grateful to all my professors in the Harold Vance Department of Petroleum Engineering at Texas A&M University for the guidance I have received in my courses and mentorship.

Finally, I would like to thank all members of my research group for their constant support and backing during difficult times. My special thanks to Harish Kumar (graduate student, Dr. Nasr-El-Din's group), for his invaluable friendship, guidance, motivation and tremendous help in reviewing my work.

NOMENCLATURE

Wt%	Weight Percentage
CT	Computed Tomography
EOR	Enhanced Oil Recovery
DI	De-ionized
in	Inches
g	Gram
cc	Cubic centimeter
md	Millidarcy
C	Tracer concentration in the core effluent samples, mg/L
C _o	Tracer concentration at the core inlet face, mg/L
ppm	Parts Per Million
Φ	Porosity (%)
K _{abs}	Absolute Permeability (md)
PV	Pore Volume (cm ³)
S _{orw}	End Point Residual Oil Saturation (fraction)
k	Base Permeability Value For Relative Permeability Curves (md)
μ_w	Water Viscosity (cp)
D	Dispersion Coefficient (cp)
\emptyset	Porosity of phase j
S _j	Saturation of phase j

α_{jk}	Mechanical dispersivity for phase j in direction k
$ u_j $	Interstitial velocity of phase j
$\nabla_k (\rho_j X_{ij})$	Concentration gradient of component i in phase j in direction k
D_{ij}^*	Molecular diffusion coefficient of component i in the phase j
F_{jk}	Tortuosity for phase j in direction k

TABLE OF CONTENTS

	Page
ABSTRACT	ii
DEDICATION	iii
ACKNOWLEDGEMENTS	iv
NOMENCLATURE.....	v
TABLE OF CONTENTS	vii
LIST OF FIGURES.....	ix
LIST OF TABLES	xi
CONTRIBUTORS AND FUNDING SOURCES.....	xii
1. INTRODUCTION AND LITERATURE REVIEW.....	1
1.1 Heterogeneity in carbonate reservoirs.....	4
1.2 Non-destructive tracer flow through porous media.....	5
1.3 Simulation Studies for carbonate heterogeneity.....	7
2. EXPERIMENTAL MATERIALS	13
2.1 Cores.....	13
2.2 Fluids.....	15
3. EXPERIMENTAL STUDIES.....	17
3.1 Rock characterization.....	17
3.2 Computed tomography scans	18
3.3 Coreflood.....	20
4. ANALYTICAL STUDIES.....	25
4.1 Coates and Smith Model	25
4.2 New modified analytical approach.....	26

5. SIMULATION STUDIES.....	29
5.1 Commercial Simulators.....	29
5.2 Fluid Model.....	31
5.3 Core Model and orientation.....	34
5.4 Boundary conditions.....	35
5.5 Inputs.....	35
5.6 Convection dispersion model.....	35
5.7 Outputs.....	41
6. RESULTS AND DISCUSSION	42
6.1 Experimental studies.....	42
6.2 Simulation studies.....	45
7. CONCLUSIONS, FUTURE WORK AND RECOMMENDATIONS.....	56
REFERENCES.....	58

LIST OF FIGURES

	Page
Figure 1: SYSTEM OF METHODS FOR RESERVOIR DESCRIPTION ACCORDING TO THE OBJECT SCALE.....	6
FIGURE 2: COREFLOOD APPARATUS FOR TRACER EXPERIMENT	21
FIGURE 3: OPTIMA 8300 ICP-OES (INDUCTIVE COUPLED PLASMA) SPECTROMETER (REPRINTED FROM THE OPTIMA 8300 MANUAL).23	23
FIGURE 4 : A HETEROGENEOUS CORE SLICED INTO I- HOMOGENEOUS LAYERS.....	27
FIGURE 5 : A GENERIC SIMULATION MODEL OF A 6 IN. X 1.5 IN. CORE	30
FIGURE 6: (A) CARTESIAN GRID SIMULATION MODEL – CMG STARS AND (B) CROSS SECTIONAL VIEW OF THE INJECTING SURFACE OF THE MODEL	34
FIGURE 7: POTASSIUM ION CONCENTRATION PROFILE OF DIFFERENT CARBONATES.....	43
FIGURE 8: CROSS SECTION CT SCAN IMAGE OF EDWARDS WHITE CARBONATE CORE AT TWO DIFFERENT POSITIONS (A) X = 2 INCHES AND (B) X = 3.2 INCHES	44
FIGURE 9: (A) POROSITY PROFILE AND (B) PERMEABILITY PROFILE INDIANA LIMESTONE AND EDWARDS WHITE	46
FIGURE 10: TRACER CONCENTRATION PROFILE OF INDIANA LIMESTONE FOR EXPERIMENTAL AND COATES AND SMITH ANALYTICAL METHOD	48
FIGURE 11: TRACER CONCENTRATION PROFILE OF INDIANA LIMESTONE FOR EXPERIMENTAL, COATES AND SMITH ANALYTICAL METHOD AND NUMERICAL SIMULATION	48

FIGURE 12: TRACER CONCENTRATION PROFILE OF EDWARDS WHITE FOR EXPERIMENTAL AND COATES AND SMITH ANALYTICAL METHOD	49
FIGURE 13: TRACER CONCENTRATION PROFILE OF EDWARDS WHITE FOR EXPERIMENTAL, COATES AND SMITH ANALYTICAL METHOD AND NUMERICAL SIMULATION	50
FIGURE 14: TRACER CONCENTRATION PROFILE OF EDWARDS WHITE FOR EXPERIMENTAL AND COATES AND SMITH ANALYTICAL METHOD	51
FIGURE 15: TRACER CONCENTRATION PROFILE OF EDWARDS WHITE FOR EXPERIMENTAL AND MODIFIED ANALYTICAL APPROACH....	51
FIGURE 16: DISPERSION COEFFICIENT PROFILE OF (A) INDIANA LIMESTONE AND (B) EDWARDS WHITE FROM THE MODIFIED ANALYTICAL APPROACH	53
FIGURE 17: EFFECT OF TIME STEPS ON THE CONCENTRATION PROFILE USING THE NEW ANALYTICAL APPROACH	54

LIST OF TABLES

	Page
TABLE 1: PETROPHYSICAL PROPERTIES OF THE INDIANA LIMESTONE, EDWARDS YELLOW AND AUSTIN CHALK CARBONATE CORES.	13
TABLE 2: PETROPHYSICAL PROPERTIES OF THE PINK DESERT, WINTERSET AND EDWARDS WHITE CARBONATE CORES.	14
TABLE 3: PHYSICAL PROPERTIES OF FLUIDS.....	16
TABLE 4: PHYSICAL CHARACTERISTICS OF CARBONATES	17
TABLE 5: EFFECT OF SIMULATION TIME STEP ON THE TOTAL RUN TIME FOR INDIANA LIMESTONE (IL_2)	55

CONTRIBUTORS AND FUNDING SOURCES

This project was supported by a thesis committee consisting of Dr. Hisham Nassr-El-Din (graduate advisor) and Dr. Jerome Schubert (committee member) from the Department of Petroleum Engineering and Dr. Mohamed El-Halwagi of the Department of Chemical Engineering.

The experiments and simulations were supervised by Harish T.A. Kumar (graduate student, Texas A&M University).

There are no outside funding contributions to acknowledge related to the research and completion of this document.

1. INTRODUCTION AND LITERATURE REVIEW

The nature of carbonate formations have been a subject of interest due to their diverse pore structure and varying permeability. Geologists have defined carbonate pore classes based on porosity-permeability relationships and sedimentology. The fluid-flow through these pore classes are still hard to characterize and help decide the method of further recovery of oil from the reservoir due to the complex internal fluid flow paths.

A tracer is an identifiable substance that can be tracked through the course of a process that provide with valuable information on the series of events in the process or the redistribution of the elements involved. In simple words, tracer is a simulator, that must be similar in behavior of the substance to identify and, yet it must be sufficiently different to be identifiable. Tracers in general are characterized as conservative (one that does not react with the reservoir) and partitioning (interacts with other fluid or rock surface in the system).

Many companies apply tracer on a routine basis. Tracers are used to identify the directional flow trends, assess the orientation and depth of perforations. They are also an important tool in providing valuable insight into the problem of short circuiting of waste water between reinjection and production wells. The reservoir engineer's problem generally is a lack of adequate information about fluid flow in the reservoir. The information obtained from tracer tests is unique, and tracer tests are a relatively cheap method to obtain this information. They also provide a method of evaluating the fracture nature of the system and thus the magnitude of the short circuiting problems. The

information is an addendum to the general field production history and is used to reduce uncertainties in the reservoir model.

Tracers can be broadly divided into two general groups:

1. Chemical Tracers
2. Radioactive Tracers

Chemical tracers are those which can be identified and measured quantitatively by general analytical methods such as conductivity, refractive index, concentration profiles and elemental spectroscopy. Radioactive tracers are detected by their emitted radiation, usually beta or gamma. This research is concerned entirely with the use of chemical non-destructive tracer.

Tracers can be further subdivided into those which can be made a part of the natural system (experiment or well under study) and those which cannot. The first group mostly includes radioisotopes of the constituent elements in the reservoir fluids, used by achieving equilibrium with their own non-reactive kinds. The second group mostly includes chemical tracers. This group of tracers has to establish equilibrium with every other kind present if they are reactive in nature. The non-destructive tracers are simpler to track and analyze since their concentration is not affected by the mineralogy of the formation rocks.

Tracer tests provide tracer-response curves that may be evaluated further to obtain relevant additional information. Adequate data presentation and simple calculations can give further knowledge about the flow behavior in the reservoir. More quantitative information can be obtained by fitting response curves obtained from

numerical simulation to the observed response curves. Additional information also can be obtained by applying analytical procedures on the basis of generic or simplified reservoir models.

The use of tracers in the reservoir studies shows that this is the best method to evaluate the downhole region of the well and inter-well space. Traditionally, the reservoir studies have combined the integration of the geological, geophysical, and well tests as well as geochemical data and production history to construct geologically realistic models. Tracer studies give new opportunities to evaluate the fluid-flow properties and continuation or compartmentalization of reservoirs.

Consequently there are two types of tracer tests: single well test and inter-well test. Single well tracer test is carried out on a borehole where the tracer is injected with a consequent direct in-situ measurement. Tracer materials may be chemical or radioactive. In the first case, the conductivity profile is measured before and after injection to evaluate place and rate of injected fluids. In the second case, after the first gamma ray logging the radioactive tracer is pumped in a borehole with a consequent detection of gamma ray distribution along the reservoir profile. In this study we will be working with conservative tracer of 8 wt% Potassium Chloride solution. Tracer can be used in several methods depending on the nature of the study. In most cases, tracers are injected into the reservoir before flooding any fluid to understand the reservoir to improve the oil recovery efficiency of the flooding process.

1.1 Heterogeneity in Carbonate Reservoirs

Arne Skauge (2006) studied the single phase dispersion by injection a slug of water tracer into carbonate rocks with different pore classes. He found that each carbonate pore class has a characteristic response to the tracer flow, which affects the breakthrough curve. However, Coats and Smith (1964) model was proposed as a good model to be used to describe single phase dispersion for a majority of different carbonate pore classes with uniform distribution. Dauba et al. (1999) conducted an experimental study to examine the effect of longitudinal heterogeneity on the tracer profile and it was found that long tail is an indication for high permeability contrast. On contrary, the profile is not sensitive to cross section heterogeneity. Spencer and Watkins et al. (1980) found that cores with a wide pore size distribution showed a higher residual saturation after CO₂ flood. On much larger scale heterogeneity, Shook et al. (2003) used the tracer test results analysis to estimate the flow geometry and heterogeneity in fractured, geothermal reservoirs.

Carbonate formations have been known to have highly complex pore structure and exhibit a wide range of pore classes, such as moldic porosity, vuggy porosity, interparticle porosity and microporosity. Ziauddin and Bize (2007) had studied the effects of pore scale heterogeneities and its application for matrix acidizing. Based on their sedimentology, various classifications have been developed by geologists.

Determining the flow pattern of any injected fluid is an important parameter to be considered while designing any oil recovery project (Ball et. al. 1983). Anatomical

investigation could not only provide an insight of reservoir heterogeneity, but also provide basic information that can be made to work to our advantage (Alpay et al. 1972).

In this study, outcrop core samples from six different carbonates are obtained and used to conduct tracer experiments. The cores were examined for uniform exterior and porosity was measured using CT scan images.

1.2 Non-destructive tracer flow through porous media

Tracing techniques have a broad application in hydrogeology and oil industry to characterize permeability along reservoir profile and flow paths in aquifer or productive reservoirs (Chopra et al. 2004).

Tracer testing has been used since early 1950s for aiding in characterizing the heterogeneity in all rock types. Several studies with dyes, brine and a surface active compound were studied by Strum and Johnson (1950).

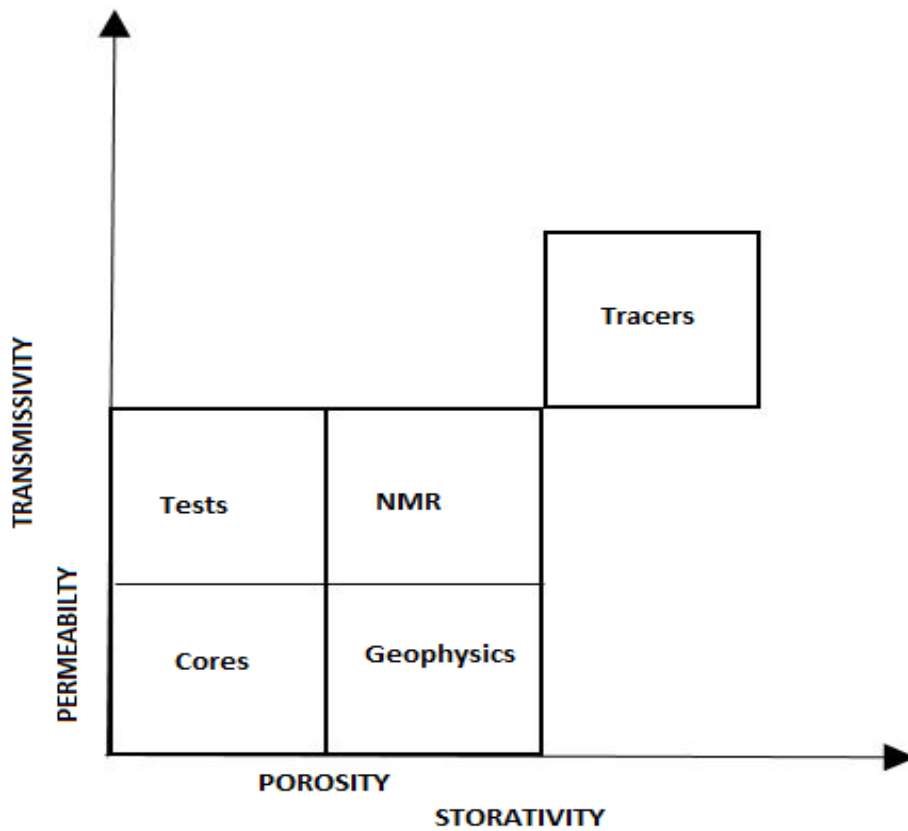


Figure 1: System of methods for reservoir description according to the object scale

For the tracer experiments, since the mobility of both potassium and chloride ions are almost the same, which minimizes the liquid junction potential, Potassium chloride is used, rather than sodium chloride. The liquid junction potential is caused when two electrolytic solutions of different concentrations are placed in contact with each other and there is a difference in the rate of migration (diffusion) of the anions and cations, causing one to pull the other along faster than the average advective speed (Steven et al. 2004).

Study conducted by Anisimov et al. (2009) provided evidence that tracer tests are highly effective in improving oil-water displacement process for Enhance Oil Recovery Process (EOR).

1.3 Simulation Studies for carbonate heterogeneity

Two core samples of six different carbonate core types using STARS simulator of Computer Modeling Group (CMG). The models are used to match the measured field data of produced tracer concentration (8wt% KCl) and to determine the main controlling parameters affecting tracer profiles.

At heterogeneous scales, where the parameters change, the Fick's law assumptions are no longer valid and the classical theory does not predict the amount of mixing. If the heterogeneity is much finer than the system size of interest, its effects can be averaged or homogenized (Panfilov et al. 2000).

For a laminar flow at steady state, the streamlines that follow the velocity field do not cross each other. Only diffusion can allow mass transfer normal to the fluid flow. The classical theory describing this spreading or dispersion, based on Fick's first and second laws, combines mass conservation and the time rate of change for the flux of a contaminant moving through a porous medium. The equations are based on the assumptions that the mixing is similar to diffusion (a statistically random process), that

the contaminant tracer is conservative (it does not react or sorb to the medium), and that the medium properties (porosity, permeability, and dispersivity) are homogeneous on the scale of measurement. Here a homogeneous material is defined as media with constant system properties that have a single characteristic length scale, l , such as a pore size or grain size that is smaller than the measurement size; $L(l < L)$. Fick's laws are generally useful only after the contaminant has traversed approximately fifty such characteristic length scales.

Another property often reported for a porous medium is dispersivity. Dispersion is known to vary with velocity, and an empirical relationship has been proposed to account for this:

$$D = \alpha v^m$$

Where D is the measured dispersion coefficient, v is the velocity, α is the dispersivity (also known as the characteristic length when the coefficient m is equal to 1) and m is an empirical exponential factor, often with a value in the range from 0.8 to 1.2 for homogeneous media.

Dispersivity attempts to factor out the velocity relationship and hence provides a single value describing the effect that a given medium has on mixing. While this relationship appears useful for homogeneous media, it is not expected to be a useful parameter in heterogeneous media, as the empirical value m changes in each new region.

Dispersion mechanisms or conditions that cause the spreading of a contaminant during flow through a porous medium may be lumped into five categories – diffusion, fluid effects, medium effects, fluid–medium interactions, and boundary/initial conditions. These mixing mechanisms or system conditions (Greenkorn, 1983) have differing effects based on the strength and direction of the fluid velocity.

Diffusion causes mixing due to random molecular motions, causing the contaminant to, on average, move from regions of high concentration to regions of low concentration. It becomes less important at larger fluid velocities as other mechanisms overwhelm diffusion.

Fluid effects (gravity, density and viscous differences between fluids, saturation levels, and turbulence) cause one fluid to move faster or in different directions than the bulk flow. The different fluids may vary simply in the contaminant amount present (causing viscosity and density difference) or may be different chemical species or mixtures of species. An important consideration is how easily the different fluids mix – miscible fluids freely mix, immiscible fluids do not mix.

Medium effects (tortuosity, auto-correlation, dead end pores and recirculation) cause spreading due to the nature and alignments of the pores. Some pores will be longer or wider and will have faster average velocities than others. This causes mixing when the

fluid in one pore reaches a downstream location at a different time than the fluid in a different pore. The pore structure may also trap some contaminant in a dead-end or recirculation zone, causing a time lag before it returns to the main flow field, which can be seen in plumes with long tails. These mechanisms may be dominant in cases of anomalous dispersion.

Fluid-medium interactions (adsorption, chemical reaction, hydrodynamics, and heterogeneity effects) cause spreading by interfering with the ability of the contaminant to pass unhindered through the pore space. Hydrodynamic dispersion is caused by friction between the fluid and the pore walls. The heterogeneity effect, the main focus of this work, changes the amount of dispersion in a variety of ways and it operates over all the time and spatial scales of interest (Sternberg et al., 1996).

Systems that have non-constant or large length scales in comparison to the scale of measurement ($l \approx L$) are called heterogeneous. At heterogeneous scales, and where the system parameters change, the Fick's law assumptions are no longer valid and the classical theory does not predict the amount of mixing. A system can be homogeneous at one length scale, heterogeneous at another and again homogeneous at some other scale. This type of system is said to have an evolving or hierarchical heterogeneity (Cushman Ginn et al., 1993).

Another modeling concern is the scale at which the system is heterogeneous. If the heterogeneity is much finer than the system size of interest, its effects can be averaged or homogenized (Panfilov et al., 2000). If the heterogeneity is at the size of the system ($l \approx L$), or larger than the system of interest ($l > L$), it is very difficult to model and it cannot be homogenized or described with an effective or averaged system parameter. There is very little information known about how such systems behave; yet these systems can be readily encountered in natural porous materials on scales of human interest. It is these large-scale heterogeneities that are examined in this work.

Many current theories for transport in heterogeneous porous media place strict limits on the nature of the heterogeneity such that properties must vary smoothly, have only small changes in property distributions, and/or that the heterogeneity length scale must be much smaller than the system size. These constrained theories may not seem realistic for all natural media, yet they offer a significant improvement from theory based on Fick's laws assumptions.

Modeling of fluid flow through a porous media is based on the below mentioned differential equation:

$$D \frac{\partial^2 c}{\partial x^2} - v \frac{\partial c}{\partial x} = \frac{\partial c}{\partial t}$$

The first term on the left is the Dispersion term that causes the ‘spreading’ of the solute through the porous media. It consists of both molecular and mechanical dispersion components which cannot be distinguished on the Darcy scale.

$$D = D_{\text{mol}} + D_{\text{mech}}$$

D Mechanical dispersion reflects the fact that not everything in the porous medium travels at the average water flow speed. Some paths are faster, some slower, some longer, some shorter. This leads in a net spreading of the solute plume that looks very much like a diffusive behavior.

Determining the dispersive properties of the porous media is necessary for achieving a highly successful enhanced oil recovery project. During such displacement of fluids, a transition zone where the concentration of the solute varies from maximum value to zero is present. The dispersion coefficient can be determined from measurements of solvent concentrations at the producer wells.

The relation between concentration and dispersion coefficient is calculated from analytical solutions to the deterministic equations modeling the process. The analytical dispersion models of tracer flow through porous media are based on the convection – dispersion equation and are restricted to cases of mixing governed by Fickian dispersion in one and two dimension porous media. Zhang et al. (1992) found that if the velocity correlation function decays slowly at large Fickian scales, the asymptotic value of the dispersion is non-Fickian.

2. EXPERIMENTAL MATERIALS

2.1 Cores

Two cylindrical cores from six different carbonate types of 1.5 in. diameter and 6 in length were cut from outcrop rocks with a core bit. To ensure a consistent permeability anisotropy range, the cores were drilled in a single direction. Table 1 and Table 2 reports the petrophysical properties of each core sample.

Core ID	IL_2	IL_3	EY_2	EY_3	AC_2	AC_3
Length (in.)	6	6	6	6	6	6
Porosity from CT images (vol %)	15.785	14.948	30.307	34.496	46.3113	37.8172
Pore Volume (cm³)	26.5	26.4	49.9	53.2	50	49.7

TABLE 1: PETROPHYSICAL PROPERTIES OF THE INDIANA LIMESTONE, EDWARDS YELLOW AND AUSTIN CHALK CARBONATE CORES.

Core ID	PD_1	PD_2	W_1	W_2	EW_1	EW_3
Length (in.)	6	6	6	6	6	6
Porosity from CT images (vol %)	21.389	25.926	18.945	18.347	16.973	16.1973
Pore Volume (cm³)	38.2	43.9	19.5	21	38.1	42.6

TABLE 2: PETROPHYSICAL PROPERTIES OF THE PINK DESERT, WINTERSET AND EDWARDS WHITE CARBONATE CORES.

Each core samples are examined for uniformity and ensured that no edges are compromised before the start of the experiment. All the dimensions are measured using a standard laboratory vernier caliper.

2.2 Fluids

2.2.1 Brines

The selection of tracer requires the following characteristics of the tracer fluid:

- a) Analytical detectability
- b) Cost
- c) Availability
- d) Safety
- e) Non-reactive nature with the reservoir minerals

The tracer fluid used in this study is 8 wt% KCl brine solution. The tracer brine were prepared by mixing reagent-grade salts with deionized water. The concentration of potassium ions in the tracer solution was measured using Inductively Coupled Plasma (ICP). The experiment was repeated three times and the average concentration of 36.68 g/L was obtained.

Typically any chloride salt could be used but potassium chloride was preferred over the easily available Sodium because the potassium and chloride ion mobilities are almost the same, which minimizes the liquid junction potential. Since the retardation force is directly proportional to the ionic mobility of the salt solution, potassium chloride is more suitable for this study.

Ionic mobility (correlates with conductivity) in water ($u / (10^{-8} \text{ m}^2\text{s}^{-1}\text{V}^{-1})$)

Na⁺: 5.19

K⁺: 7.62

Cl⁻: 7.91

The liquid junction potential is caused when two electrolytic solutions of different concentrations are placed in contact with each other and there is a difference in the rate of migration (diffusion) of the anions and cations, causing one to pull the other along faster than the average advective speed (Steven P. K. et al. 2004) . The physical properties of the fluids were measured in the laboratory and are listed below:

	Density (g/cm³)	Viscosity (cp)
8 wt% KCl	1.048	1.072
DI Water	0.9972	1

TABLE 3: PHYSICAL PROPERTIES OF FLUIDS

3. EXPERIMENTAL STUDIES

3.1 Rock Characterization

Two cylindrical cores of 1.5-in. diameter and 6-in. length were drilled from each of the six rock types. Six carbonate rock types were studied: Indiana Limestone, Edwards yellow, Pink Desert, Edwards white, Winterset and Austin Chalk.

Rock type	Characterization
Indiana Limestone	High storage capacity, good permeability
Austin Chalk	Fine pores and micro-pores
Pink Desert	Not as well connected as Indiana Limestone
Edwards Yellow	More moldic pores than Pink Desert
Winterset Limestone	High storage capacity and low permeability
Edwards White	Smaller pores and less connectivity

TABLE 4: PHYSICAL CHARACTERISTICS OF CARBONATES

3.2 Computed Tomography Scans

Operating Principle

A CT scan image of a porous material is shown in the image below. In this method note a rock example is used.

Parameter of interest in this study is the porosity, which will be obtained from the data acquired from each slice of the image scanned.

Image analysis consists of a sequence of steps that will be explained in this section. First we choose an appropriate volume of Interest (VOI) and image segmentation. The region of interest (ROI) refers to the selected region, on a single cross-section image. The volume of interest (VOI) refers to the integration of all the ROIs across all the selected image levels, and defines the sub-volume of the dataset within which procedures will be performed such as model construction and morphometric calculation.

Tools are provided for highly flexible volume of interest (VOI) delineation. As example a dataset of a porous rock is chosen for which a cylindrical shape is applicable. This 8-bit reconstructed image contains 256 grey values. Each voxel has grey-scale intensity from 0 to 255. For morphometric analysis, a binary format image is needed. To this end each pixel needs to become either black or white. This procedure is called segmentation. For simple segmentation, a user must define a threshold value.

A closed pore in 3D is a connected assemblage of space (black) voxels that is fully surrounded on all sides in 3D by solid (white) voxels. Percent closed porosity is the

volume of closed pores as a percent of the total of solid plus closed pore volume, within the VOI. An open pore is defined as any space located within a solid object or between solid objects, which has any connection in 3D to the space outside the object or objects. Total porosity is the volume of all open plus closed pores as a percent of the total VOI volume.

Procedure

The scan was performed according to the following steps:

1. Cores are labeled with the Injection and Production side in order to identify the direction of flow while performing the experiment.
2. The cores are laid on the testing tray which is then automatically moved into the scanner. The core is cropped digitally to obtain the exact dimensions of the core.
3. The lamp is initialized and the scanner initializes. Once the lamp reaches the minimum value,

3.3 Coreflood

Setup

Figure 2 presents the schematic diagram of the coreflood apparatus. The components of this setup are listed as follows:

1. A three in. vertically mounted stainless steel core holder, with a rubber sleeve within for applying overburden pressure on the core.
2. Three accumulators for storing oil, CO₂ and brine.
3. An ISCO Syringe pump used for injecting fluids into the core at specified rates or pressures.
4. A pressure transducer to monitor pressure drop across the core.
5. A N₂ cylinder for applying overburden pressure on core and back pressure at core outlet.
6. A hydraulic oil pump to inject hydraulic oil into a cavity between the internal surface of the core holder and the rubber sleeve, for balancing applied overburden pressure on core.
7. The complete flow circuit is checked once again for any possible leaks in the system to avoid experimental errors.
8. A LABVIEWTM software to record pressure drop measured by the pressure transducer with time.
9. A heating oven containing the core holder, to perform experiments at reservoir temperatures.

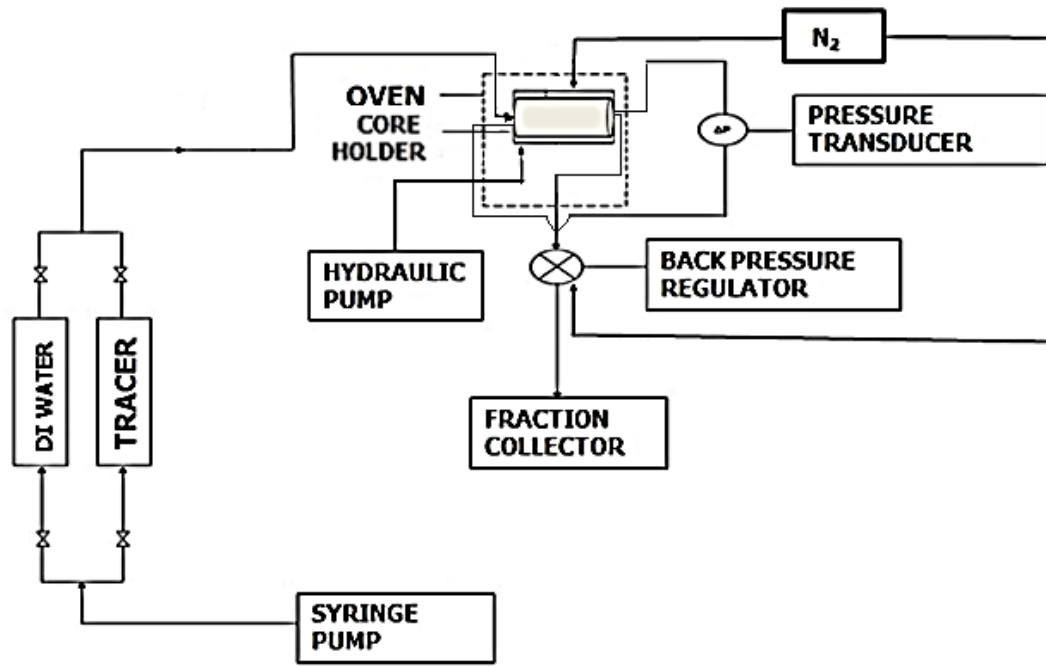


FIGURE 2: COREFLOOD APPARATUS FOR TRACER EXPERIMENT

Preparation of Cores

Following were the procedures. A summary of the core preparation experiments listing initial core properties appears in Tables 1 and 2:

1. Three different cores of each of the six types that are used in this study were dried in an oven at 250°F for a period of 48 hours, and weighed to obtain the dry weight of the core.
2. The cores were saturated with DI water in a saturation cell for 10 days to achieve complete saturation to obtain the wet weight for measuring the pore volume of the cores.
3. Absolute permeability measurements were conducted on these eighteen cores by flooding DI water at low constant rates of 0.5, 1 and 2 cm³/min, ensuring 100% water saturation, and then the permeability was calculated using Darcy's law at the stabilized pressures for each rate. The experiments were conducted at room temperature, with an overburden pressure of 1100 psi and a back pressure at core outlet of 500 psi.
4. Pore volume and porosity values were calculated via material balance.
5. Tracer fluid was injected into the cores for four pore volumes.
6. Core effluent samples were collected and analyzed by Inductively Coupled Plasma (ICP-OES) for K⁺ concentration.

Optima 8300 ICP-OES Spectrometer, shown in Figure 3, is to analyze core effluent samples for the total potassium ion concentrations was used. Knowing the total

amount of potassium ions injected, the volume and the potassium ions concentration for each collected sample, the adsorption for potassium ions in the carbonate cores was determined. It was found that the adsorption of the ions on the carbonate rock surface was negligible and did not affect the tracer experiments results.



FIGURE 3: OPTIMA 8300 ICP-OES (INDUCTIVE COUPLED PLASMA) SPECTROMETER (REPRINTED FROM THE OPTIMA 8300 MANUAL)

Tracer Sampling

After initiating the tracer flow using a syringe pump remotely using LABVIEW™, the following steps are carried out for collecting the samples at the production end of the coreflood apparatus.

1. The core effluent samples were collected at a predetermined time interval based on the calculations from the pore volume and tracer flow rate.
2. The tracer flow rate was set as 3cc/min and samples were collected every minute until four pore volumes were injected from the accumulator.
3. After the effluent samples were collected, the samples were analyzed for K⁺ ion concentration using ICP.
4. The adsorption of Potassium ions on carbonate surface was negligible from the experimental data and did not affect the results obtained for the tracer experiments.
5. The dead volume in the system was calculated at 5.136 cc.
6. The tracer dispersion in the tubing and fittings was negligible compared to the core samples and therefore, were ignored from the calculations.

4. ANALYTICAL STUDIES

4.1 Coates and Smith Model

The convection dispersion model characterized by the fundamental equation written below:

$$\frac{\partial C}{\partial t} = D \frac{\partial^2 C}{\partial x^2} - u \frac{\partial C}{\partial x}$$

An analytical solution for the convection dispersion model by Laplace transformation and then inversion was obtained, subject to the following initial and boundary conditions:

At $t = 0$, $C(x, 0) = 0$ for $x \geq 0$

(Initial Conditions)

At $x = 0$, $vC_0 = vC - D(\partial C/\partial x)$

And, as $x \rightarrow \infty$, $C(\infty, t) = 0$

(Boundary conditions)

The resulting solution (Coates and Smith 1964) was given by the equation below:

$$C/C_0 = \frac{1}{2} \operatorname{erfc} \left(\frac{\sqrt{y}}{2} \frac{1-1/f}{\sqrt{1/f}} \right) - \frac{\sqrt{1/f}}{\sqrt{\pi y(1+1/f)}} e^{-y(1-1/f)^2/(41/f)} \left(1 - 2 \frac{1/f}{1+1/f} \right)$$

$$\gamma = ul/D$$

Where,

D is dispersion coefficient.

I is the pore volumes injected.

f is the flowing pore volume fraction.

l is the core length.

u is the interstitial velocity.

4.2 New Modified Analytical Approach

In this section, a detailed workflow is explained to discuss the modified analytical approach which is developed by using an existing equation stated by Zhang et al. (1992) with the Coates and Smith Model for characterizing heterogeneous carbonates.

From literature, we have a well-established Coates and Smith model which is in a very good solution to characterize homogeneous carbonates and is used widely across the industries. In this study, a heterogeneous carbonate core outcrop of Edwards White is sliced into layers (using the CT scan data) and each individual slice (each slice of characteristic length $x_i = 0.1$ cm) is considered as an individual homogenous medium with a fixed porosity.

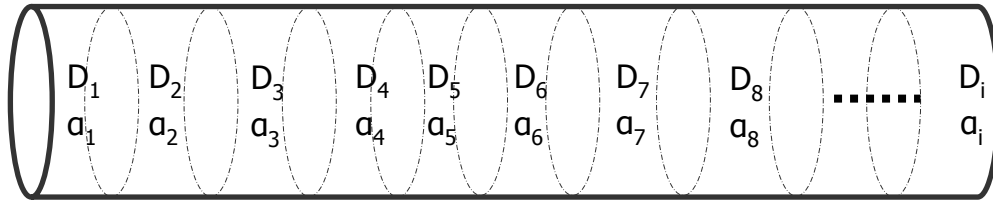


FIGURE 4 : A HETEROGENEOUS CORE SLICED INTO I- HOMOGENEOUS LAYERS

The following is the workflow to obtain the relating variables to utilize the Coates and Smith Model:

$$\varphi(x_i) \longrightarrow k(x_i)$$

The permeability profile of the core is calculated using the Carmen-Kozeny Equation from the porosity profile obtained from the CT scan of the core since the pressure gradient is constant across the length, and this data is validated using the pressure drop data from the numerical simulation results. The velocity of the fluid is measured at each layer using the injection velocity and a function of permeability profile.

$$u(x_i) = f(k_i)$$

$$u(x_i) = u_{oi} \left[1 + \frac{x_i}{l} \right]^\beta$$

The characteristic length (x_i) can be expressed as:

$$x_i = \bar{v} t$$

The relation for calculating $U(x_i)$ can be re-written as :

$$u(v\bar{t}) = u_{oi} \left[1 + \frac{\bar{v}t}{l} \right]^\beta$$

Using this velocity calculated at every x_i , dispersion coefficient is calculated using:

$$D(vt) = \int_0^t u(v\tau) d\tau$$

The final solution for the above integral was given by Zhang et al. (1992):

$$D(vt) = \frac{u_{oi}}{v} \left(\frac{1}{1 + \beta} \right) \left[\left(1 + \frac{vt}{l} \right)^\beta - 1 \right]$$

The vt values from the Zhang's equation and the Pore Volume Injected data from the Coates and Smith Model for homogeneous solution are combined to calculate the dispersion coefficient for each individual layer. Since there is minimal effect on molecular dispersion of fluid solute through porous media, mechanical diffusivity can be calculated as $\alpha = D/u$. This dispersion coefficient calculated is the validated using numerical simulation using a commercial simulator.

5. SIMULATION STUDIES

5.1 Commercial Simulators

The purpose of a simulation model is to establish a clear understanding of the results obtained from the experiments and discuss the validity of the analytical results in generating the tracer profiles of the carbonate cores. Using the results from these simulations, future prediction strategies can be developed and guide us in real-time operations (both field-scale or in laboratory scale).

STARS, an advanced processes reservoir simulator developed by Computer Modeling Group Ltd., include the option to simulate tracer experiments along with other chemical processes. A wide range of grid and porosity models in both the field and laboratory can be simulated and is one of the best program that can be used for this study.

STARS require a dataset with all the initial parameters and respective values assigned as an input. Based on the user command, the simulator runs the initialized model and generates the desired output.

Thus STARS model calibrated with that of the experimental results would be ideal in modeling complex EOR processes, to save runtime and maintain accuracy. During each tracerflood experiment, the injection tracer concentration and injection pressure was maintained constant throughout the experiment, in a DI water saturated in the cores.

A generic 3D model of a core is shown below (Figure 4):

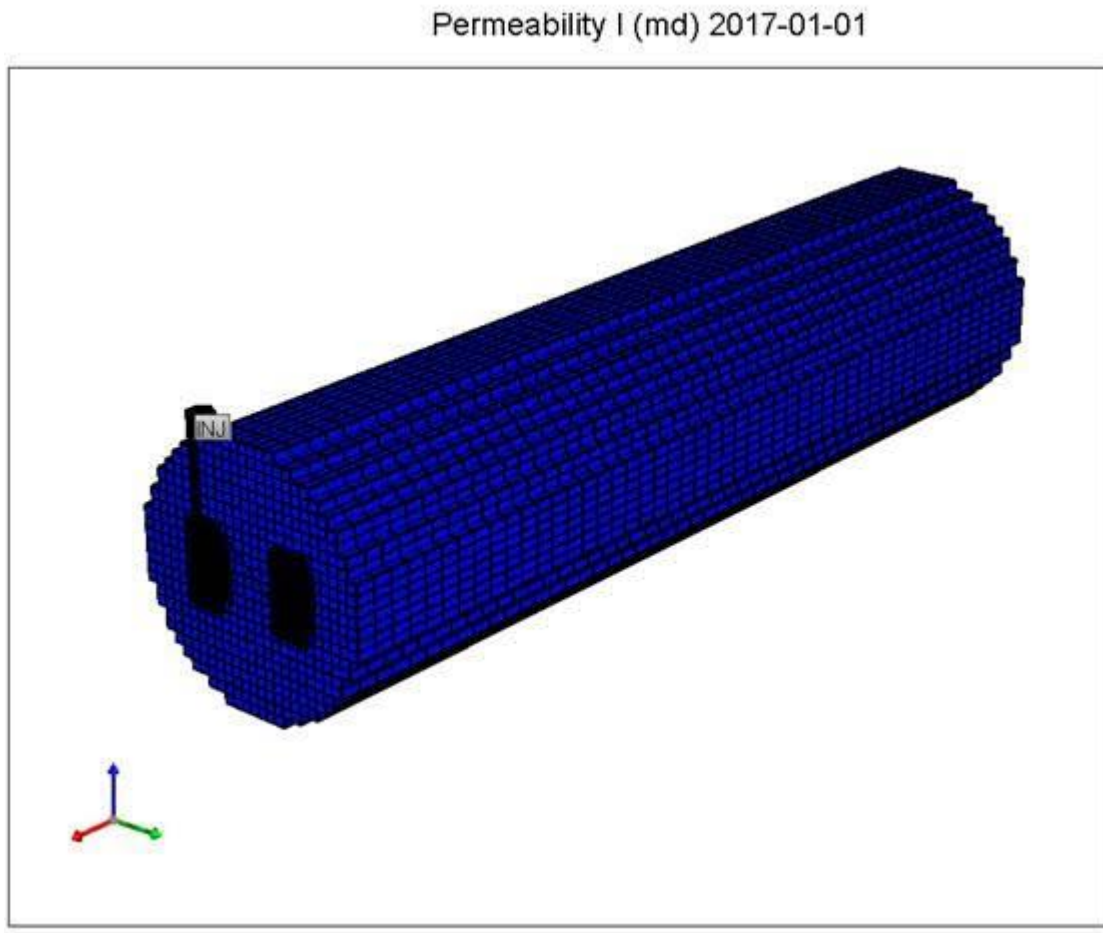


FIGURE 5 : A GENERIC SIMULATION MODEL OF A 6 IN. X 1.5 IN. CORE

Using the BUILDER from the CMG Launcher, we select the STARS simulator and the single porosity model mode for our study. The model is created in the Cartesian system with 100 x 25 x 25 cells in i-j-k directions. After creating this model, the outer cells are initialized with null values to obtain a cylindrical model with outer cells which does not allow the fluid flow to leak (acts as a boundary for the system)

5.2 Fluid Model

The tracer experiments aims to develop and reproduce the experiments carried out in the laboratory. There are only two fluids used in the experiments- DI Water and 8wt% KCl tracer solution.

Tracer experiments provide with learning about the separate, tortuous paths of fluid phase(s) through a porous medium. These factors are scale dependent and cannot be generalized for a large scale reservoir based on the outcrop data. The selection of the tracer is such that they partition into a single phase and does not interact with the other phases present in the medium of study. They are mainly used to yield well to well communication and studying the reservoir heterogeneity.

In CMG STARS, the following keywords are used for modeling tracer based simulations:

a) DIFFL_WAT

$$(\emptyset S_j D_{ij}^*/F_{jk})$$

Effective molecular diffusion coefficients (cm^2/min) of water phase in I direction (since the effect of molecular diffusion is very negligible and therefore, J, K components equals to zero).

b) *TORTU(*INCPORSAT)

Tortuosity is a ratio that characterizes the convoluted pathways of fluid diffusion and electrical conduction through porous media.

Enables the option for Tortuosity (formation resistivity) which defines the molecular diffusion coefficients entered using *INCPORSAT factor, ($\emptyset S_j$)

The total molecular flux of component i in the phase j in the direction K due to diffusion is given by:

$$J_{ijk} = (\emptyset S_j D_{ij}^* / F_{jk}) \nabla_k (\rho_j X_{ij})$$

Where,

\emptyset – Porosity of phase j

S_j – Saturation of phase j

D_{ij}^* – Molecular diffusion coefficient of component i in the phase j

F_{jk} – Tortuosity for phase j in direction k

$\nabla_k (\rho_j X_{ij})$ – Concentration gradient of component i in phase j in direction k

c) MDISPI_WAT

Mechanical dispersivity (cm) in the phase for the i, j, k directions.

The mechanical dispersion flux J_{ijk} of the component i in phase j in direction k is given by:

$$J_{ijk} = \emptyset S_j \alpha_{jk} |u_j| \nabla_k (\rho_j X_{ij})$$

Where,

\emptyset – Porosity of phase j

S_j – Saturation of phase j

α_{jk} - mechanical dispersivity for phase j in direction k

$|u_j|$ - interstitial velocity of phase j

$\nabla_k (\rho_j X_{ij})$ – Concentration gradient of component i in phase j in direction k

d) DISPI_WAT

Effective total dispersion coefficients (cm^2/min) of the water phase for the i direction.

The total dispersive flux J_{ijk} of component i in phase j i direction k is given by:

$$J_{ijk} = -D_{ijk} \nabla_k (\rho_j X_{ij})$$

Where,

$-D_{ijk}$ – Total dispersion coefficient of component i in phase j in direction k

$\nabla_k (\rho_j X_{ij})$ – Concentration gradient of component i in phase j in direction k

Total dispersion is made up of two parts: Effective Molecular diffusion (component and phase dependent) and mechanical dispersion (which is a property of the rock).

5.3 Core Model and Orientation

A Cartesian grid 3-D model was created using CMG STARS, using 100 cells along the X axis, 25 cells along Y axis and 25 cells along Z axis. The cells are labeled as (x,y,z) based on the i-j-k positions. The model is oriented horizontally (identical to the coreflood experiments) and hence the flow of fluids are along the X-axis.

The fluid is injected into all cells along the cross section of the Y-Z axes and producer was set at the opposite face (end of the core)

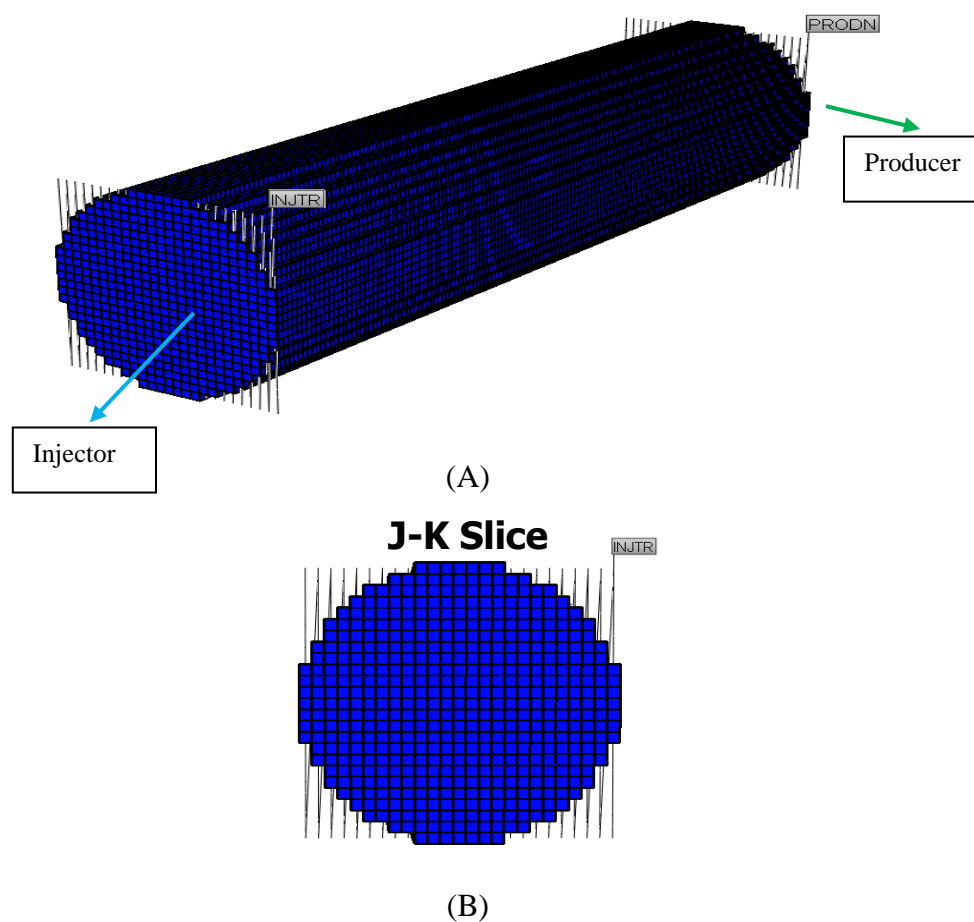


FIGURE 6: (A) CARTESIAN GRID SIMULATION MODEL – CMG STARS AND (B) CROSS SECTIONAL VIEW OF THE INJECTING SURFACE OF THE MODEL

5.4 Boundary Conditions

No flow zones were established at all the boundaries, other than the cell boundaries in which the wells have been completed. This ensured that the fluid flow was contained within the core model to prevent any leak via boundary cells, and depicted the net flow of fluids from the injector to the producer, similar to the experiments performed.

5.5 Inputs

The rock porosities and isotropic permeabilities are used for the core model properties. The fluid properties of the tracer were accounted in the simulation model using the tracer feature of the CMG STARS simulator. The model is initialized by enumeration, with pressures in all cells being set at the experimental back pressures, and the connate water saturations uniformly set across the model. Since this study used homogenous cores, the initial saturation and porosity profiles were uniform along the lengths of the core model.

5.6 Convection Dispersion Model

The fundamental mass balance equation is

$$\sum I + \sum P - \sum O - \sum L = \sum A \quad (1)$$

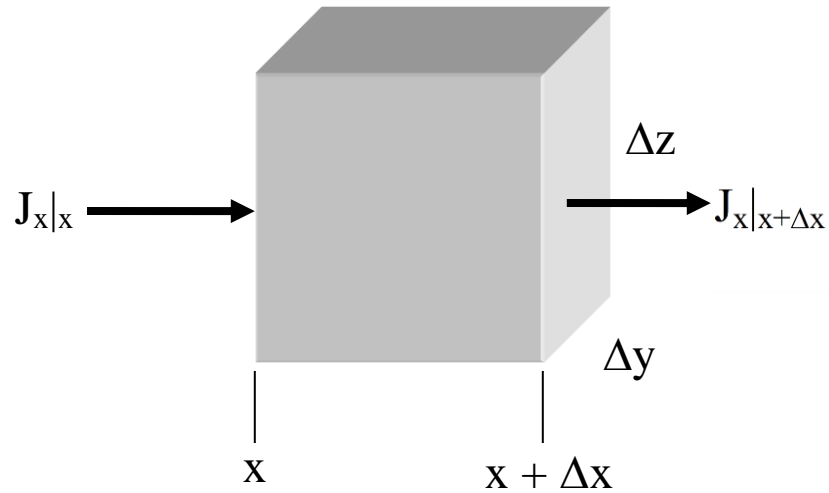
Where:

- I = inputs
- P = production
- O = outputs
- L = losses
- A = accumulation

Assume that no chemical is produced or lost within the control volume and hence $\Sigma P = \Sigma L = 0$. So (1) simplifies to

$$\sum I - \sum O = \sum A \quad (2)$$

Considering a control volume cell where there is flux in the x direction only, we have



Where $J_{x|x}$ indicates the mass flux density ($ML^{-2}T^{-1}$) in the x direction at the point x.

In order to satisfy (2), we must have

$$(J_{x|x} - J_{x|x+\Delta x})\Delta y\Delta z = \frac{\partial C}{\partial t}\theta\Delta x\Delta y\Delta z \quad (3)$$

That is, the flux into the left wall times the area over which it occurs, minus the flux out of the right wall times its area in any interval of time Δt must equal the change in chemical mass in the control volume.

The flux J_x has two components; there is an advective component J_c and a dispersive component J_d . The flux of solute due to convection is $J_c = v\theta C$. Dispersion mimics diffusion in the sense that the dispersive flux appears to be driven by concentration gradients (e.g., $\partial C/\partial x = 0.001 \text{ mg/cm}^4$), and can be expressed using the same mathematical form as Fick's law for diffusive flux:

$$J_d = -D^* \frac{\partial C}{\partial x} \quad (4)$$

where J_c and J_d are areal fluxes ($\text{ML}^{-2}\text{T}^{-1}$) and D^* is the dispersion coefficient (L^2T^{-1}).

Incorporating the two flux components into equation (3), we have

$$\left(v\theta C \Big|_x - D^* \frac{\partial C}{\partial x} \Big|_x - v\theta C \Big|_{x+\Delta x} + D^* \frac{\partial C}{\partial x} \Big|_{x+\Delta x} \right) \Delta y \Delta z = \frac{\partial C}{\partial t} \theta \Delta x \Delta y \Delta z \quad (5)$$

Dividing both sides by $\theta \Delta x \Delta y \Delta z$ gives

$$\frac{\left(vC \Big|_x - \frac{D^*}{\theta} \frac{\partial C}{\partial x} \Big|_x - vC \Big|_{x+\Delta x} + \frac{D^*}{\theta} \frac{\partial C}{\partial x} \Big|_{x+\Delta x} \right)}{\Delta x} = \frac{\partial C}{\partial t} \quad (6)$$

Or, collecting terms containing v and D^* and assuming that v , θ , and D^* are constant in space, we have

$$v \frac{(C|_x - C|_{x+\Delta x})}{\Delta x} + \frac{D^*}{\theta} \left(-\frac{\partial C}{\partial x} \Big|_x + \frac{\partial C}{\partial x} \Big|_{x+\Delta x} \right) = \frac{\partial C}{\partial t} \quad (7)$$

Shrinking Δx to differential size, the first term is simply $-v \partial C / \partial x$. In the second term, we are obviously just taking the gradient of the gradients, and if we shrink Δx to differential size we have

$$-v \frac{\partial C}{\partial x} + \frac{D^*}{\theta} \frac{\partial \left(\frac{\partial C}{\partial x} \right)}{\partial x} = \frac{\partial C}{\partial t} \quad (8)$$

or equivalently,

$$-v \frac{\partial C}{\partial x} + D \frac{\partial^2 C}{\partial x^2} = \frac{\partial C}{\partial t} \quad (9)$$

It is customary to replace D^* / θ with D . This is the 1-D version of the CDE.

Based on the above derived 1-D equation, Coates and Smith developed a model.

An analytical solution for the convection dispersion model by Laplace transformation and then inversion was obtained, subject to the following initial and boundary conditions:

at $t = 0$, $C(x, 0) = 0$ for $x \geq 0$ (Initial Conditions)

at $x = 0$, $vC_0 = vC - D(\partial C/\partial x)$ and as $x \rightarrow \infty$, $C(\infty, t) = 0$ (Boundary conditions)

The resulting solution (Coats and Smith 1964) was given by Eq. xx:

$$C/C_0 = \frac{1}{2} \operatorname{erfc} \left(\frac{\sqrt{\gamma} (1 - I/f)}{2 \sqrt{I/f}} \right) - \frac{\sqrt{I/f}}{\sqrt{\pi \gamma (1 + I/f)}} e^{-\gamma (1 - I/f)^2 / (4I/f)} \left(1 - 2 \frac{I/f}{1 + I/f} \right) \dots\dots 2$$

$$\gamma = ul/D$$

where D is effective dispersion coefficient, I is the pore volumes injected, f is the flowing pore volume fraction, l is the core length, u is the interstitial velocity. If the effect of molecular diffusion is negligible compared to the mechanism of dispersion, the dispersion coefficient can be simplified to a widely accepted linear relationship, $D = \alpha u$, where α is the mechanical dispersivity coefficient.

5.7 Outputs

Each core flood experiment was simulated using the respective inputs as described above. Two different models were tested in this study. The results plotted were the concentration profile of each model. The diffusion coefficient is also calculated from the equation from Zhang et .al (1998), which is subsequently used to calculated a corrected concentration profile for the carbonates.

6. RESULTS AND DISCUSSION

6.1 Experimental Studies

The tracer experiments were conducted on each core for each carbonate rock type to study the flow behavior and obtain same normalized tracer concentration profile. The normalized tracer (C/C_0) in the core effluent samples for different carbonate rock types is plotted as a function of the cumulative pore volume injected.

For Indiana limestone carbonate rock type, the tracer concentration profile was found to be symmetrical at one pore volume injected. These results are expected because carbonates of well-connected inter-granular pores exhibit a symmetrical profile around 1 PV injection at $(C/C_0)=0.5$ (Skauge et al. 2006). The tracer profile is dominated by a low fraction of inaccessible pores and no capacitance effect (no dead-end pores).

For other carbonate rock types, the pores are not as well connected as for Indiana limestone carbonate rock type. Consequently, it is believed that the fluid flows in a smaller fraction of the pore volume in these carbonates than in well-connected Indiana limestone. The tracer concentration profiles that show an early breakthrough and long tail behavior confirm this hypothesis. The behavior of the tracer concentration profiles is believed to be due to preferential flow paths for the tracer fluid through the porous media. The tracer concentration profiles appear consistent with the observation of thin sections.

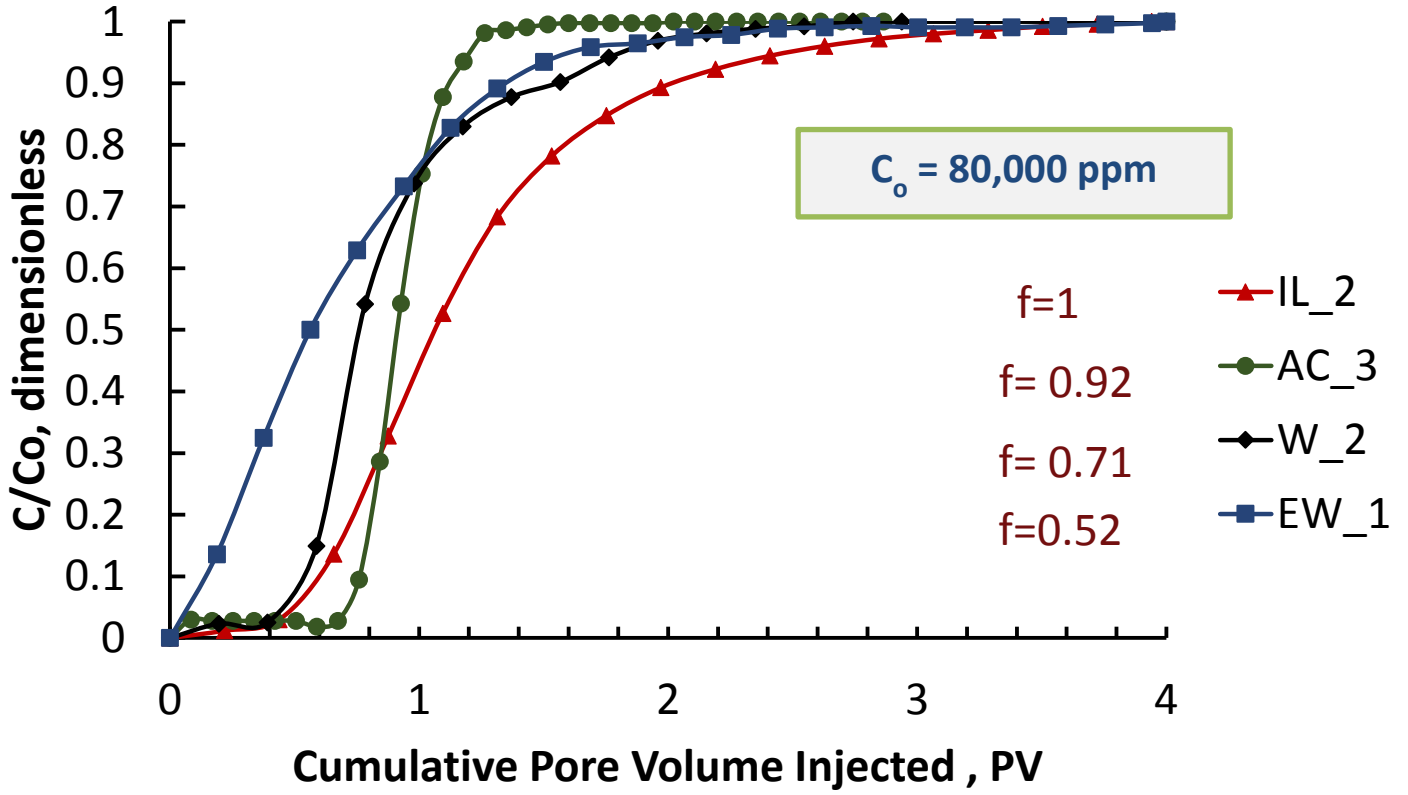


FIGURE 7: POTASSIUM ION CONCENTRATION PROFILE OF DIFFERENT CARBONATES

As shown in the figure 6, the resulting profile was found to be symmetrical about $C/C_0 = 0.5$ at one pore volume injected, i.e., conservation of mass. These results are expected because carbonates of inter-particle pore class exhibit symmetrical profile around 1PV injection at $C/C_0 = 0.5$ (Skauge et al. 2006). The absence of adsorption effects was also indicated by the breakthrough of the $0.5C_0$ point in the tracer test at one pore volume injected.

For Indiana Limestone, the normalized tracer concentration $C/C_0 = 0.5$ reaches when 1 PV of tracer fluid is injected into the core. Identically the value of flowing fraction is

0.92 for Austin Chalk, which is also homogeneous in nature, is less homogeneous compared to Indiana Limestone. For Edwards White, the tracer reached normalized tracer concentration of 0.5 at a much less value of pore volume of tracer injected (0.52 PV) which clearly indicates that this carbonate type is highly heterogeneous. This is also observed from the porosity profile of the core which has a large variation in the total porosity value.

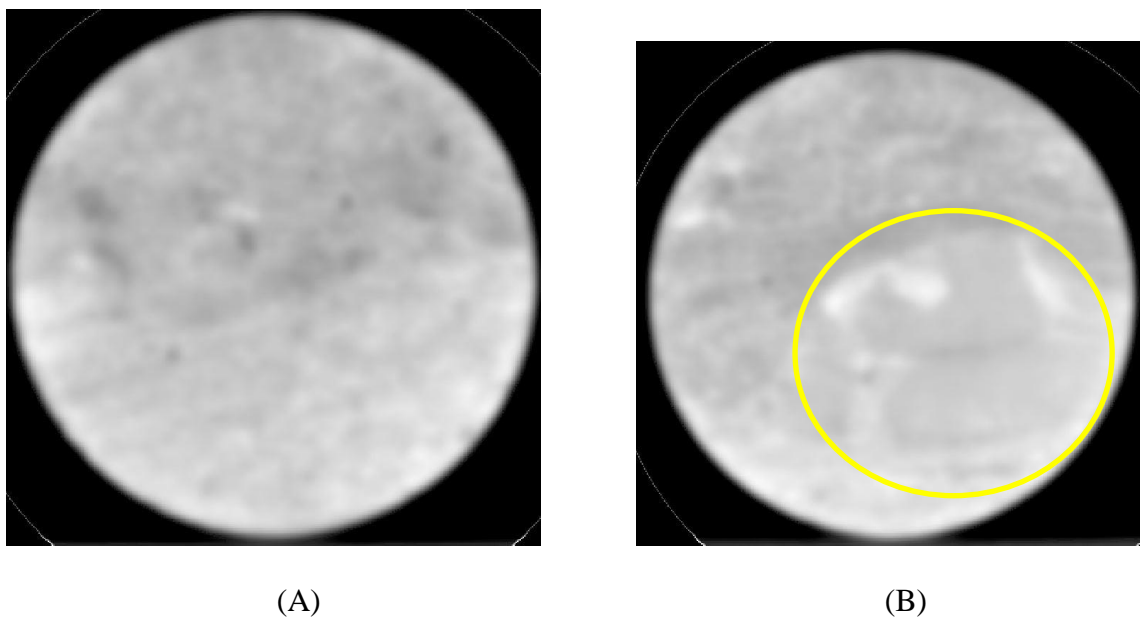


FIGURE 8: CROSS SECTION CT SCAN IMAGE OF EDWARDS WHITE CARBONATE CORE AT TWO DIFFERENT POSITIONS (A) X = 2 INCHES AND (B) X = 3.2 INCHES

The region in the yellow circle clearly indicates the presence of large vugs within this carbonate core.

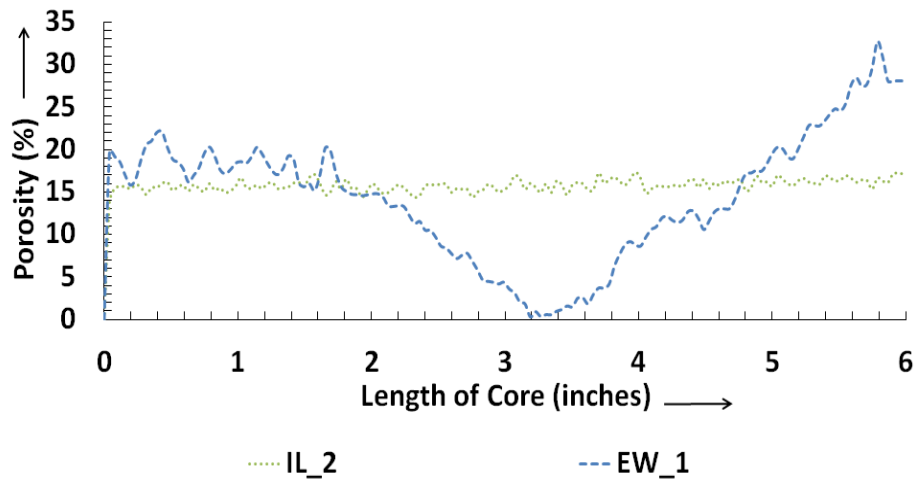
From the tracer concentration profiles, we can observe the difference in the time taken to reach the maximum concentration is because of the structural difference in all the carbonate types (all the cores used in the experiment have the same physical

dimensions. Indiana Limestone is known to have well interconnected pores and good storage capacity, whereas Edwards Yellow has smaller pores with more moldic pores.

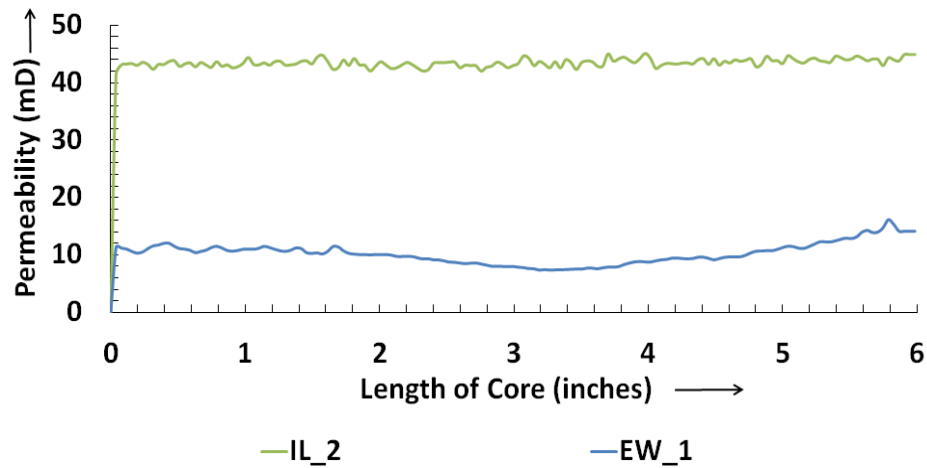
The S-shape concentration profile shown in the concentration profiles is attributed to two mechanisms. First, repeated collisions with water molecules generate microscopic random spreading of tracer molecules that, over time, are observable at larger scales. This random motion results in net movement of tracer particles from regions of high concentration to regions having low concentration. This process is a process by which the concentration gradient diminishes by time, and is called Diffusion. Second, the complex pore structure results in flowing fluid to take a tortuous path. Variations in local velocity in magnitude and direction along tortuous flow paths cause tracer particles to spread. This is called mechanical dispersion. These mechanisms cause the concentration profile of the tracer coming out from the core became S-shape, and any change in diffusion, dispersion and the fraction of the total pore volume occupied by the mobile fluid affect this profile.

6.2 Simulation Studies

Two best core cases, one for each homogeneous and heterogeneous carbonate. Based on the experimental results, Indiana Limestone (IL_2) was selected for the homogenous carbonate type. Similarly, Edwards White (EW_1) was selected for the heterogeneous carbonate type. The selection was strictly based on the nature of the tracer flow and concentration profile of the carbonates and the time taken to achieve a normalized tracer concentration. The porosity and permeability were in accordance with the above mentioned profiles.



(A)



(B)

FIGURE 9: (A) POROSITY PROFILE AND (B) PERMEABILITY PROFILE INDIANA LIMESTONE AND EDWARDS WHITE

As seen from Fig 8 (A) and (B), we can conclude that Indiana Limestone has a very uniform porosity distribution across the length of the core and the same is reflected in the permeability that was calculated using the Carmen – Kozeny Equation.

$$K(\phi) = K_o * [\phi / \phi_o]^{**ckpower} * [(1 - \phi_o) / (1 - \phi)]^{**2}$$

For the heterogeneous case, Edwards White carbonate core was selected based the same two parameters and the nature of the concentration profile and the flowing fraction.

In the next section, the homogeneous and heterogeneous cases are explained in detail.

Homogeneous Carbonate

The numerical simulation run was initialized and the total dispersion coefficient of 3.42 cm²/min from the Coates and Smith model. The resulting concentration profile is plotted in comparison with the experimental data in Figure 10. As we can see, the Coates and Smith solution is an almost perfect fit to the experimental data and this is validated using a commercial numerical simulator.

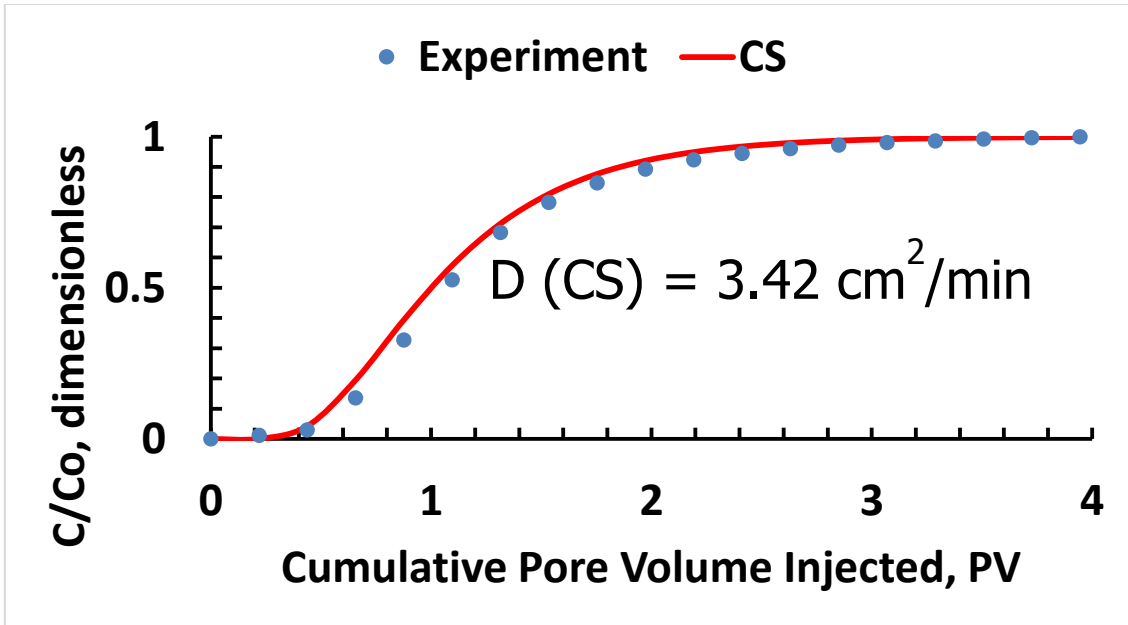


FIGURE 10: TRACER CONCENTRATION PROFILE OF INDIANA LIMESTONE FOR EXPERIMENTAL AND COATES AND SMITH ANALYTICAL METHOD

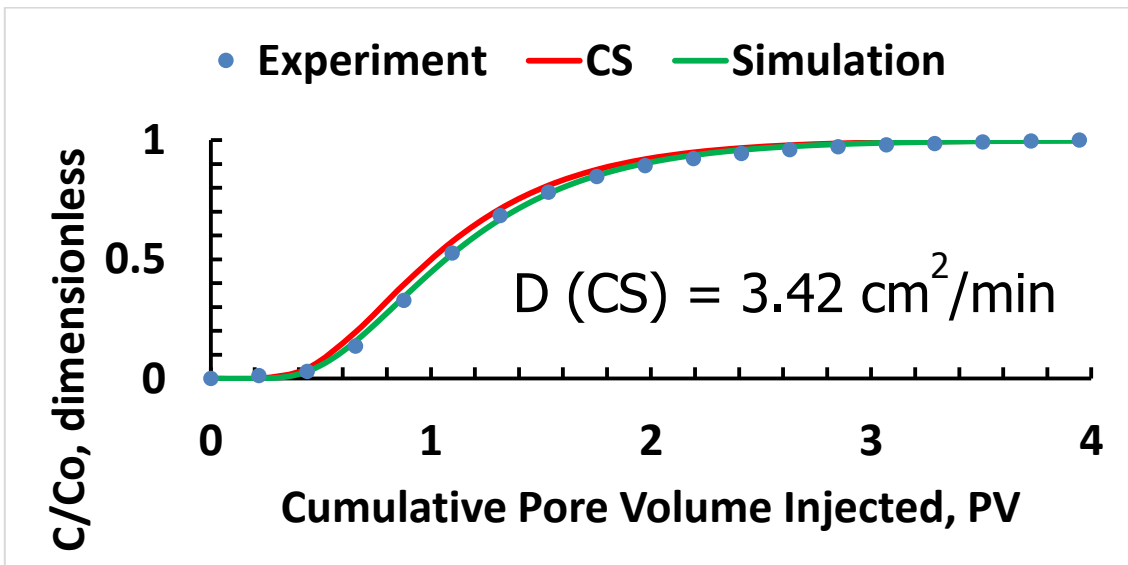


FIGURE 11: TRACER CONCENTRATION PROFILE OF INDIANA LIMESTONE FOR EXPERIMENTAL, COATES AND SMITH ANALYTICAL METHOD AND NUMERICAL SIMULATION

Heterogeneous Carbonate

The Coates and Smith Model is used to compare with the experimental model and the result fits for a high value of $D = 160 \text{ cm}^2/\text{min}$ as seen in the figures below:

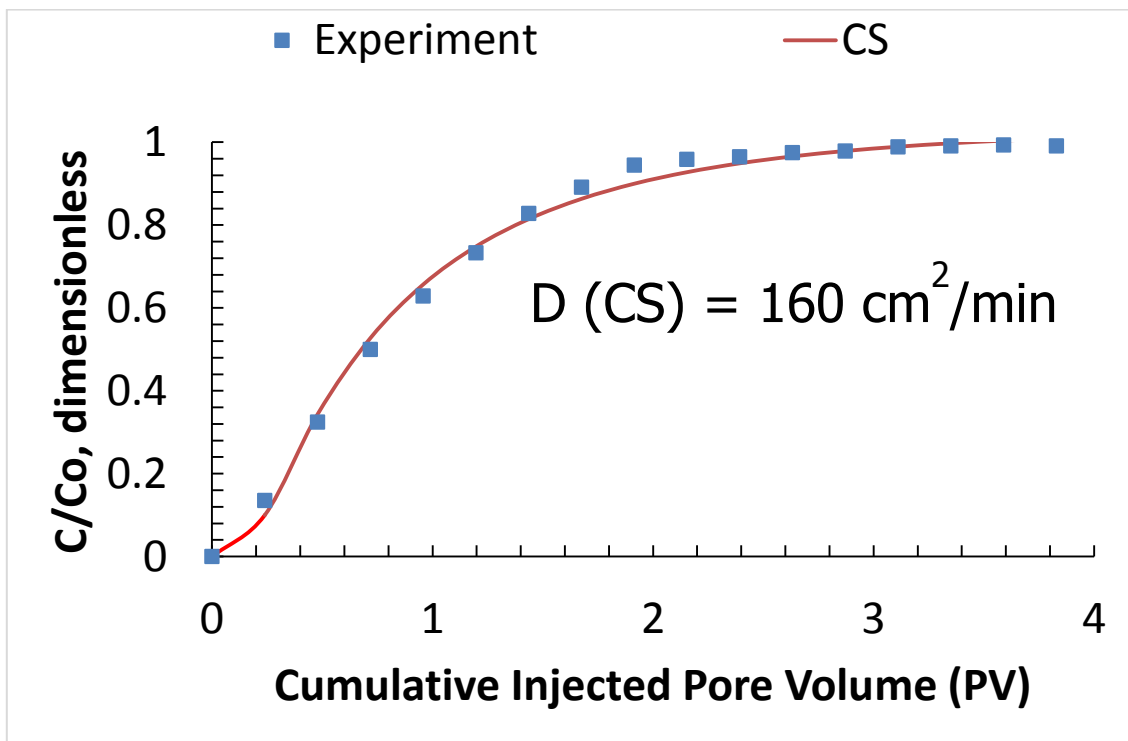


FIGURE 12: TRACER CONCENTRATION PROFILE OF EDWARDS WHITE FOR EXPERIMENTAL AND COATES AND SMITH ANALYTICAL METHOD

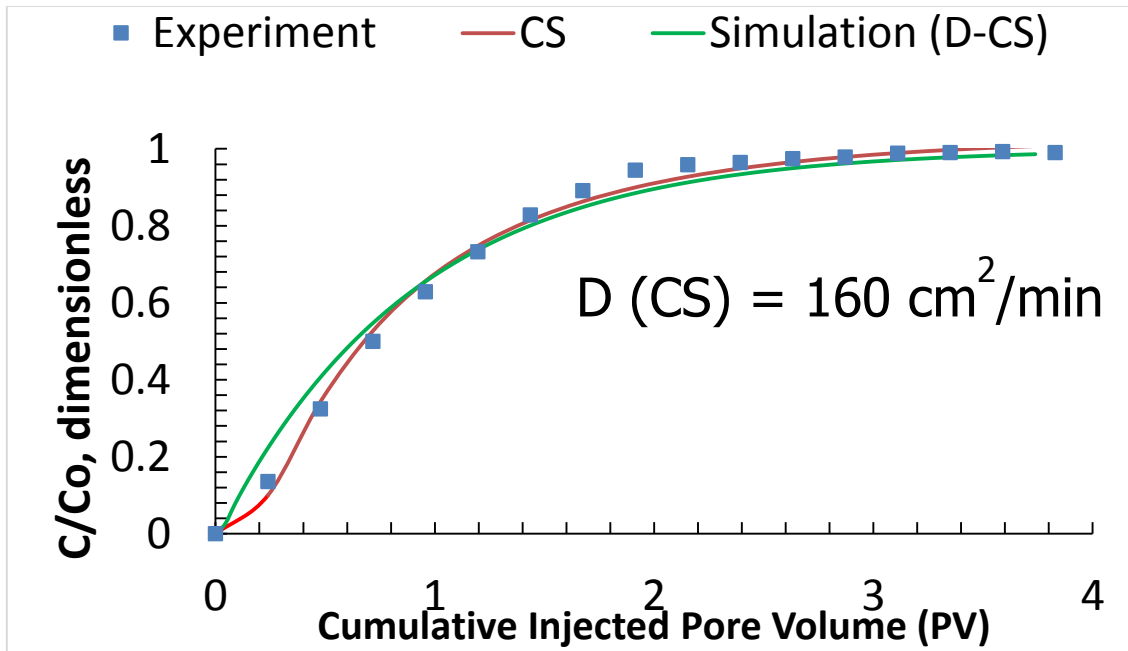


FIGURE 13: TRACER CONCENTRATION PROFILE OF EDWARDS WHITE FOR EXPERIMENTAL, COATES AND SMITH ANALYTICAL METHOD AND NUMERICAL SIMULATION

The new modified approach (discussed in section 4.2) predicts a concentration profile as shown in Figure 14. This is also a near perfect fit to the experimental data.

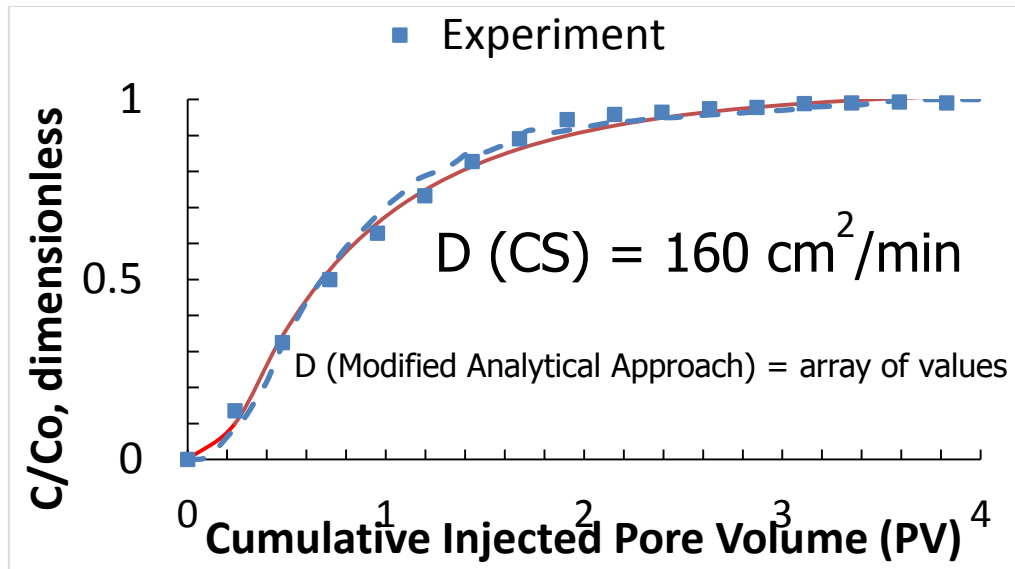


FIGURE 14: TRACER CONCENTRATION PROFILE OF EDWARDS WHITE FOR EXPERIMENTAL AND COATES AND SMITH ANALYTICAL METHOD

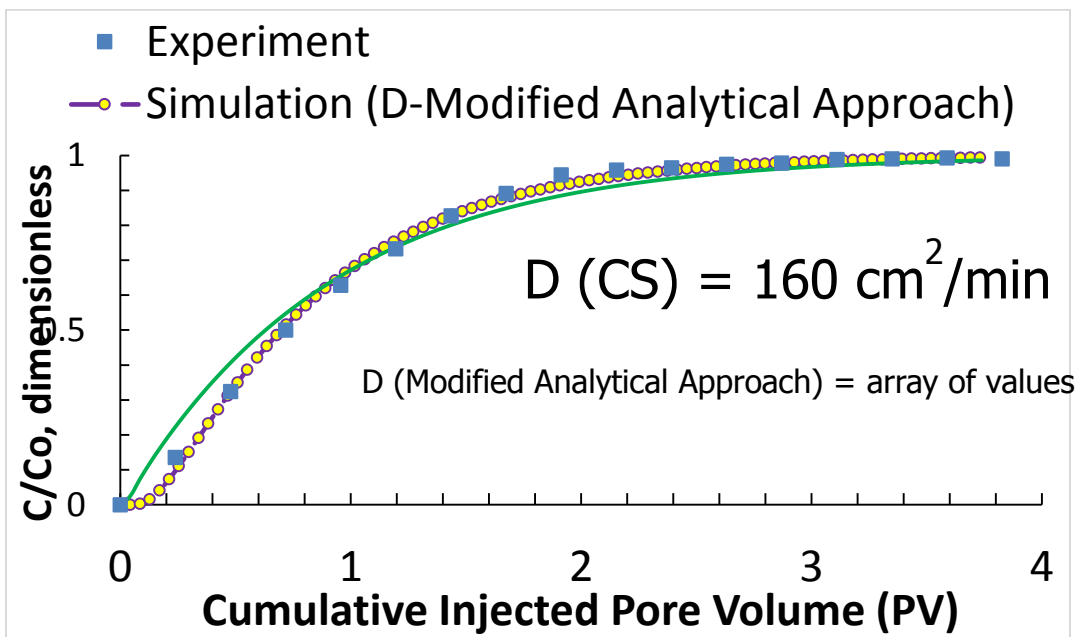
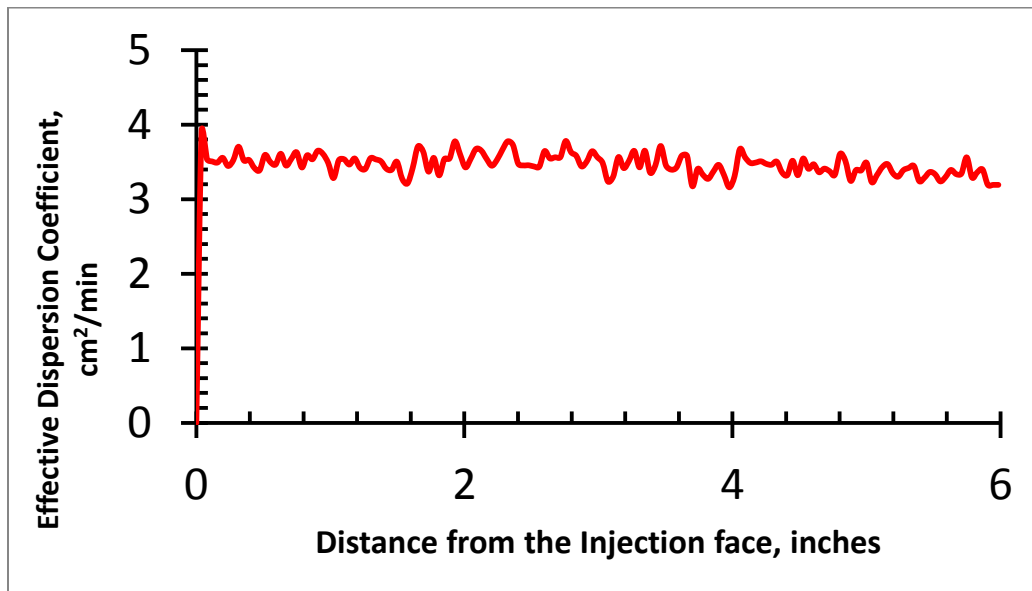


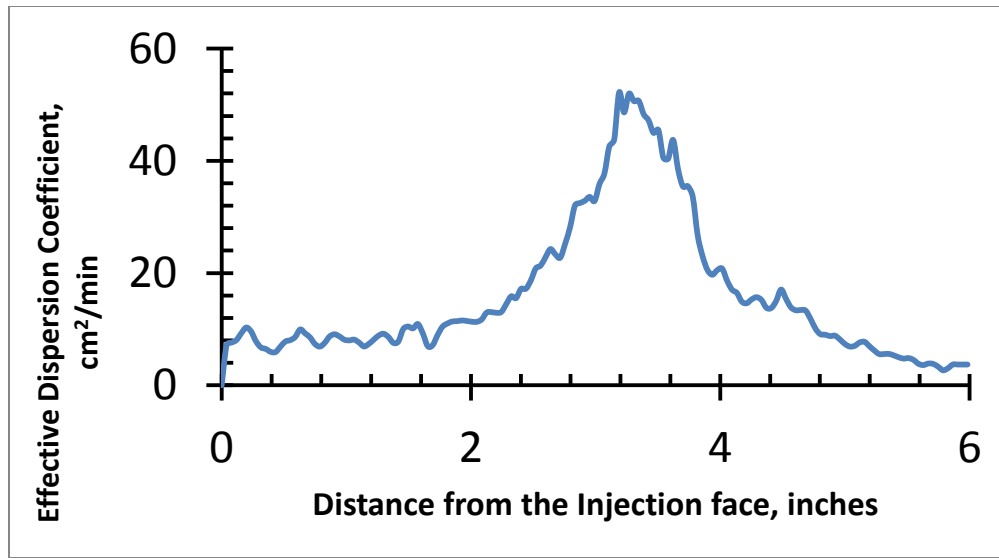
FIGURE 15: TRACER CONCENTRATION PROFILE OF EDWARDS WHITE FOR EXPERIMENTAL AND MODIFIED ANALYTICAL APPROACH

The numerical simulator then uses the new modified approach and calculates the concentration profile and the result was a perfect match. The curve passes almost all the experimental data points and the values of effective dispersion coefficient predicted were realistic.

The dispersion coefficient calculated using the modified analytical approach was validated. For the simulation study, the value of $D = 3.42 \text{ cm}^2/\text{min}$ and the effective dispersion coefficient profile (Figure 16(A)) for homogeneous carbonate (Indiana Limestone) is in accordance with the assumed value, which proves that Coates and Smith Model is a good model for characterizing homogeneous carbonates.



(A)



(B)

FIGURE 16: DISPERSION COEFFICIENT PROFILE OF (A) INDIANA LIMESTONE AND (B) EDWARDS WHITE FROM THE MODIFIED ANALYTICAL APPROACH

The value of $D = 160 \text{ cm}^2/\text{min}$ was assumed for conducting the numerical simulation based on the Coates and Smith Model and the resulting concentration profile was a decent fit, but this value of D is very high. So, using the new analytical approach, the effective dispersion coefficient is calculated and plotted (Figure 16(B)). This clearly shows the value of D varies between $5\text{-}55 \text{ cm}^2/\text{min}$, which is not remotely close to the unrealistic high value predicted by Coates and Smith Model. This shows that heterogeneous carbonates cannot be characterized using the traditional Coates and Smith Model. This new analytical approach presented in this study is good method to study and characterize the heterogeneous carbonates.

Sensitivity Study

Time Step of simulation

To check the benefits of the new analytical approach, sensitivity on the time step is studied in this section. A simulation sensitivity case was performed to mimic the Indiana Limestone core (IL_2) by decreasing the sampling time step to 0.5 seconds.

The notable observation in this experiment was the run time for the simulation.

Two different time steps, 30 seconds and 0.5 second, are used to simulate and the concentration profile that was obtained are shown below:

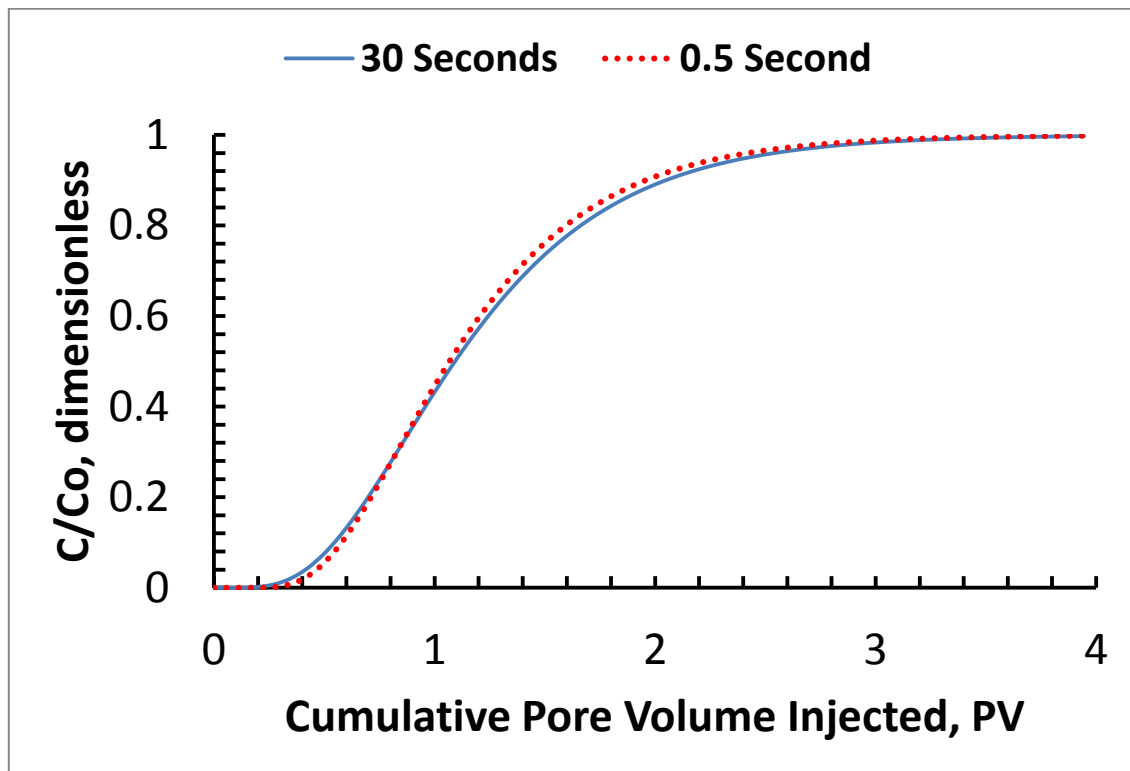


FIGURE 17: EFFECT OF TIME STEPS ON THE CONCENTRATION PROFILE USING THE NEW ANALYTICAL APPROACH

SIMULATION TIME STEP (sec)	TOTAL RUNTIME (min)
30	1:36
0.5	32

TABLE 5: EFFECT OF SIMULATION TIME STEP ON THE TOTAL RUN TIME FOR INDIANA LIMESTONE (IL_2)

The result of this simulation run was not very prominent compared to the original simulation except for a slight variation in the C/C_o 'S Curve'.

This leads us to the conclusion that the change in sampling time would not have a great influence on the results. This information is very useful for running simulation for field case tracer study for heterogeneous carbonate fields. However, reducing the time step in a laboratory scale experiment can help us with much better information with higher accuracy.

7. CONCLUSIONS, FUTURE WORK AND RECOMMENDATIONS

This study included an integrated experimental and analytical method on studying the effect of tracer flow through heterogeneous carbonate cores. The following are the conclusions of this study:

1. Applying Coates & Smith analytical solution in tracer studies toward heterogeneous media characterization gives unrealistic coefficient values.
2. Modified method presented to estimate accurate coefficient values for heterogeneous media.
3. Validation of tracer studies via numerical simulation is a must.
4. Large time steps can be cost effective in field tracer simulation studies
5. Based on β value comparison, heterogeneous case portrays stronger Fickian dispersion.

This study has provided us with science based evidence that aids in characterizing heterogeneous carbonate reservoirs based on the total diffusion of the tracer component through the porous media. The existing models did not completely account for the components of diffusion – molecular and mechanical and therefore, yields a better fit to the experimental results for heterogeneous reservoirs. The following are some recommended pathways to apply the results of this study:

1. Analyze the effect on a 20in. heterogeneous core of the selected carbonate type and observe the effect of length on the concentration profile and the results from the new modified analytical approach.

2. Reduce lab sampling time and observe the change in the nature of the 'S curve' on the experimental concentration profiles.
3. Utilize core-specific coefficient values generated, and workflow adopted in this study, for carbonate core-acidizing projects and improve the accuracy of the effect of mechanical dispersion.
4. Apply methodology developed in this study for future lab & field tracer projects for better economics.

REFERENCES

- Alpay, O.A. A Practical Approach to Defining Reservoir Heterogeneity. DOI: 10.2118/3608-PA
- Anisimov, L. The Use of Tracers for Reservoir Characterization. Society of Petroleum Engineers. DOI: 10.2118/118862-MS.
- Arya, A., Hewett, T.A., Larson, R.G. Dispersion and Reservoir Heterogeneity. DOI: 10.2118/14364-PA
- Azim, S.A., Al-Ajmi, H., Rice, C. Reservoir Description and Static Model Build in Heterogeneous Mauddud Carbonates: Raudhatain Field, North Kuwait. Society of Petroleum Engineers. DOI: 10.2118/81524-MS.
- Ball, J.T. and Pitts, M.J. Simulation of Reservoir Permeability Heterogeneities with Laboratory Corefloods. Society of Petroleum Engineers. DOI: 10.2118/11790 MS.
- Coats, K.H. and Smith, B.D. Dead-End Pore Volume and Dispersion in Porous Media. DOI: 10.2118/647-PA
- Cushman, J. H. and Ginn, T. R. Nonlocal Dispersion in Media with Continuously Evolving scales of heterogeneity, *Transport in Porous Media* 13, 123–138.
- Dauba, C., Hamon, G., Quintard, M., and Cherblanc, F., 1999, Identification of Parallel Heterogeneities with Miscible Displacement, SCA Annual Symposium, Proceedings: Society of Core Analysts. SCA 9933
- Greenkorn, R. A., Haring, R. E., Johns, H. O. and Shallenberger, L. K., Flow In Heterogeneous Hele–Shaw Models, *Petroleum Trans. AIME* 231.

Koroteev, D.A., Dinariev, O., Evseev, N. Application of Digital Rock Technology for Chemical Eor Screening. Society of Petroleum Engineers. DOI: 10.2118/165258-MS.

Lee, W.J., Sidle, R.E., and McVay, D. Reservoir Simulation: A Reliable Technology? Society of Petroleum Engineers. DOI: 10.2118/146524-MS.

Lucia, F.J. Petrophysical Parameters Estimated from Visual Descriptions of Carbonate Rocks: A Field Classification of Carbonate Pore Space. DOI: 10.2118/10073-PA

Maheshwari, P. and Balakotaiah, V. 3d Simulation of Carbonate Acidization with Hcl: Comparison with Experiments. Society of Petroleum Engineers. DOI: 10.2118/164517-MS.

Numbere, D.T. and Erkal, A. A Model for Tracer Flow in Heterogeneous Porous Media. Society of Petroleum Engineers. DOI: 10.2118/39705-MS.

Panfilov, M. 2000. Macroscale Models of Flow Through Highly Heterogeneous Porous Media. Theory and Applications of Transport in Porous Media: Springer, Dordrecht. Original edition. ISBN.

Pederson, K. S. and Christensen, P. L. 2007. Phase Behavior of Petroleum Reservoir Fluids, first edition. Boca Raton: CRC/Taylor & Francis.

Pourmohammadi, S., Hetland, S., Spildo, K. Fluid Flow Properties of Different Carbonate Pore Classes. Society of Petroleum Engineers. DOI: 10.2118/111433 MS.

Sanni, M., Abbad, M., Kokal, S. Reservoir Description Insights from an Inter-Well Chemical Tracer Test. Society of Petroleum Engineers. DOI: 10.2118/188060 MS.

- Shook, G.M., Pope, G.A., and Asakawa, K. Determining Reservoir Properties and Flood Performance from Tracer Test Analysis. Society of Petroleum Engineers. DOI: 10.2118/124614-MS.
- Sinha, R., Asakawa, K., Pope, G.A. Simulation of Natural and Partitioning Interwell Tracers to Calculate Saturation and Swept Volumes in Oil Reservoirs. Society of Petroleum Engineers. DOI: 10.2118/89458-MS.
- Skaauge, A., Sorvik, A., Vik, B., and Spildo, K. Effect of Wettability on Oil Recovery from Carbonate Material representing different pore classes. Society of Core Analysts. SCA2006-01.
- Smith, E.L., Mervyn, L., Muggleton, P.W. 1964. Chemical Routes to Coenzyme B12 and Analogues*. Annals of the New York Academy of Sciences 112 (2): 565-574. DOI: 10.1111/j.1749-6632.1964.tb45032.x
- Steven P. K. Sternberg. "Dispersion Measurements in Highly Heterogeneous Laboratory Scale Porous Media." *Transport in Porous Media* 54.1 (2004):107-124.
- Sternberg, S. P. K., Cushman, J. H. and Greenkorn, R. A., Laboratory observation of Non-local dispersion, *Transport in Porous Media* 23, 135–151.
- Sternberg, S.P.K. and Minn Univ, D. 2004. Dispersion Measurements in Highly Heterogeneous Laboratory Scale Porous Media. *Transport in Porous Media* 54 (1): 107-124.